Available online at www.sciencedirect.com
ScienceDirect
Journal of Power Sources 162 (2006) 1053–1059
JOURNAL OF POWER SOURCES
www.elsevier.com/locate/jpowsour

Yttria-stabilized zirconia thin films deposited on NiO–$(Sm_2O_3)_{0.1}(CeO_2)_{0.8}$ substrates by chemical vapor infiltration

Kenji Kikuchi [a,*], Fuminori Tamazaki [a], Koji Okada [a], Atsushi Mineshige [b]

[a] *Department of Materials Science, The University of Shiga Prefecture, 2500 Hassaka, Hikone, Shiga 522-8533, Japan*
[b] *Department of Applied Chemistry, University of Hyogo, 2167 Shosha, Himeji, Hyogo 671-2201, Japan*

Received 6 August 2006; received in revised form 20 August 2006; accepted 23 August 2006
Available online 18 September 2006

Abstract

Fabrication of YSZ films deposited on NiO–samaria-doped ceria (SDC) substrate was studied by the chemical vapor infiltration method (CVI). A NiO–SDC substrate was used as oxygen source. The main mechanism of YSZ growth was electrochemical vapor deposition (EVD), while the contribution of oxygen in the carrier gas increased with increasing NiO content of the substrate above 60.6 mol%. The YSZ film on SDC used as the anode proved effective in obtaining high cell performance. In particular, a YSZ film thickness of 1 μm yielded the highest cell performance in the temperature range from 973 to 1073 K. The CVI method was useful for preparing a dense and strong YSZ film on the complex-shaped NiO–SDC substrate.

Keywords: Yttria-stabilized zirconia; Nickel oxide; Samaria-doped ceria; Chemical vapor infiltration; Chemical vapor deposition; Electrochemical vapor deposition

1. Introduction

Solid oxide fuel cells (SOFCs) have been regarded as promising power generation systems with high efficiency. An effective solid electrolyte has been required for the practical use of SOFCs at low temperatures of about 873–1073 K. Fabrication of a thin and dense solid electrolyte is important for this purpose. Ogumi et al. employed the chemical vapor deposition (CVD) method, utilizing a porous NiO substrate as oxygen source, and electrochemical vapor deposition (EVD) processes, and showed that it is feasible to fabricate uniform, complex-shaped YSZ films on the surface of the NiO substrate [1–6]. Mineshige et al. succeeded in fabricating a micro-tube of YSZ 100 μm in diameter by the CVD–EVD process using a surface oxidized NiO wire as a substrate [3]. Pulsatile pressure change during CVI is known to allow fabrication of uniform films on complex-shaped substrate surfaces. The growth rate of the YSZ film with the chemical vapor infiltration (CVI) method has been reported to be four times as high as that with conventional CVD method [7], and this technique was used for preparing a hollow fiber of YSZ film using a NiO wire as oxygen source [8]. Ceria-based electrolytes are known to have high oxide ion conductivity, and have been regarded as a means to achieving a reduced operation temperature in SOFCs [9]. Mineshige et al. reported that a dense ceria-based film on porous substrates was fabricated by a vapor-phase deposition method similar to EVD, and elucidated the growth mechanism of ceria and ceria-SDC substrates [10]. The bare SDC layer is not used as an electrolyte for SOFCs since SDC is reduced by hydrogen through mixed-ion conduction [11,12]. Matsui et al. showed the feasibility of suppressing the electronic conduction by reducing the operation temperature and using the high oxygen partial pressure obtained by high fuel humidification, and demonstrated cell performance with a 10 μm-thick electrolyte of SDC, which yielded a high efficiency of about 0.61 at 673–873 K [13]. An YSZ film coating the surface of the SDC layer acts as an electron-blocking layer enhancing the output voltage. Particles dispersed in the YSZ matrix electrolyte reduced the overall internal resistance of the cell and gave a higher cell performance than cells with SDC or YSZ electrolyte [14]. The solid-state reaction with SDC and YSZ at the fabrication temperature, which leads to the deterioration of cell performance, has to be avoided. Tsai and Barnett prepared a 0.5 mm yttria-doped ceria layer between the YSZ and Ni–YSZ anode by reactive sputter deposition and observed a high power

* Corresponding author. Tel.: +81 749 28 8370; fax: +81 749 28 8592.
E-mail address: kikuchik@mat.usp.ac.jp (K. Kikuchi).

0378-7753/$ – see front matter © 2006 Elsevier B.V. All rights reserved.
doi:10.1016/j.jpowsour.2006.08.023

density [15]. To avoid the solid-state reaction, Wang et al. examined the fabrication of the cell component by sputtering [16]. They reported that the SDC layer had a more active site within a certain thickness in itself. However, it is difficult to prepare a complex-shaped electrolyte in order to increase the triple phase boundary, which is the most important factor in improving the fuel cell performance.

The CVI method is expected to enable the fabrication of the complex-shaped electrolyte and the solid-state reaction between SDC and YSZ could be avoided easily since the fabrication of the YSZ/NiO–SDC composite film was obtained at 1273 K with the CVI method. The deposition of YSZ films on a NiO–ceria substrate surface by the CVI method using $ZrCl_4$ and YCl_3 as metal sources and NiO–ceria as oxygen source at 1273 K were examined in our previous paper [17]. The resultant films were transparent cubic crystals of YSZ having sufficient mechanical strength for use as a free-standing solid oxide electrolyte. The growth mechanism of the YSZ film was found to be the EVD process. The aim of the study was to determine the change in the growth mechanism of YSZ film on NiO–SDC with the NiO content of the substrate in order to improve mechanical strength and cell performance.

2. Experimental

Cerium(III) nitrate (99.9% purity, Wako Junyaku), samarium nitrate (99.9% purity, Wako Junyaku), citric acid (99.9% purity, Wako Junyaku), NiO (99.9% purity, ca. 7 mm, Kojundo Chemical Laboratory), ethyleneglichol (99.9% purity, Wako Junyaku) and Polyfuron (PTFE, Daikin) were used for preparing a SDC and a NiO–SDC pellets. A SDC powder used for pellet was prepared by pechimi method [18]. A SDC powder was pressed at 250 MPa and sintered at 1573 K for 3 h to obtain the first stage SDC pellet. Next, the pellet was smashed by a mill, pressed at 250 MPa and sintered at 1773 K for 3 h. Finally, 3 g of SDC powder and 0.15 g of polyfuron as binder were mixed, pressed at 250 MPa to form a pellet 20 mm in diameter and sintered at 1873 K for 18 h. The apparent density of SDC pellet was ca. 66.4% of the theoretical density. The density was measured using a density meter (Accyupyc 1330, Micrometrics) with helium gas, yielding 96.2% of the theoretical value. A NiO–SDC pellet was prepared by sintering the mixture of SDC powder and NiO powder at 1773 K for 10 h. In this case, SDC powder was prepared by smashing the SDC pellet obtained with the pechimi method. Tetrachlorozirconium, $ZrCl_4$ (99.9% purity, 2 g, Kojundo Chemical Laboratory), trichloroyittrium, YCl_3 (99.9% purity, 2 g, Kojundo Chemical Laboratory), were used as metal sources. The CVI apparatus consisted of a reactor, vaporizers, substrate port and heater, as reported in a previous paper [7]. YCl_3 was placed on a vaporizing port in the reactor set at 1053 K, and $ZrCl_4$ was vaporized at 493–513 K. Metal chloride gases were carried with Ar or Ar containing 10 ppm hydrogen. A NiO–SDC substrate set on the substrate port was heated to 1273 K. The flow rate of the carrier gas was adjusted to 100, 200 and 400 $cm^3\ m^{-1}$ (STP) using control valves and flow meters. The argon contained 0.2 ppm oxygen and 5.3 ppm water as impurity. The pressure profile during each CVI operation was as follows: first, the total pressure in the reactor was reduced to 600 Pa in 5 s by an oil rotary vacuum pump. Then, the carrier gas was introduced into the reactor through a control valve in 1 s, and the pressure in the reactor increased. The pressure was maintained constant for 6 s, and subsequently reduced to 600 Pa to start the next 12 s cycle. The mass of $ZrCl_4$ and YCl_3 that evaporated during the CVI or CVD operations was determined by weighing the container set in the vaporizer before and after each reaction. X-ray diffraction (XRD) (Philips, X'pert-MPD) using Cu Kα was employed to analyze the thin films deposited on the NiO–SDC pellets. Their morphology was observed by a scanning electron microscope (SEM) (Hitachi, S-3200N). The growth rate of the YSZ films was estimated by measuring the film thickness using the SEM and an electron probe micro analyzer (EPMA) (Horiba, EMAX-5770W). A fuel cell was used to measure the electrical properties in similar fashion to that reported by Matsumoto et al. [19]. Pt paste was used for both the anode and cathode. The fuel cell temperature was varied from 873 to 1173 K in increments of 100 K. A pure hydrogen gas humidified at 303 K was used as fuel and a pure oxygen gas used as oxidant. Impedance measurements were carried out with a frequency analyzer (Model 5080, NF Electric Instrument) and a potentiostat (HZ-3000, Hokutodenko).

3. Results and discussion

Pulsatile pressure change during the CVI operation is thought to allow fabrication of uniform films on complex-shaped substrate surfaces. First, we investigated the fabrication of a thin YSZ film on the wall of a hole 1 mm in diameter and 20 mm in length. Fig. 1 shows an SEM image and EPMA line analysis of the cross-section of the hole. The hole could not be filled completely with resin before SEM measurement so that the hole identified in the SEM image is not the hole constructed in the SDC substrate. The line analysis along line A about Ce indicated that there was no SDC in the hole and the line analysis about Zr indicated that zirconium was present on the wall of the hole, which suggested the formation of YSZ film along the hole wall at 10 mm from the edge of the pellet.

An SEM image of the cross-section of the YSZ/SDC composite and the surface of the YSZ film deposited on SDC by the CVI method are shown in Fig. 2. The SEM image (a) of the cross-section of the YSZ film deposited on the SDC substrate revealed a dense structure. The surface of the YSZ thin film deposited on the SDC substrate at a deposition time of 20 min appeared uniform as shown in the image (b) and that of the film deposited in 80 min indicated the growth of the YSZ crystal as shown in the image (c).

Fig. 3 shows XRD patterns of a YSZ film deposited on SDC substrate at a deposition time of 20 and 80 min. Several peaks were assigned to YSZ and SDC. Intensity of the peaks assigned to SDC decreased with increasing deposition time, corresponding to the increase in the thickness of the YSZ film with deposition time.

Table 1 tabulates the Y_2O_3 contents obtained with the two types of carrier gas. A carrier gas composed of pure argon gave a low content despite the high vaporizing temperature of YCl_3. An argon carrier gas containing 10 ppm hydrogen was found to

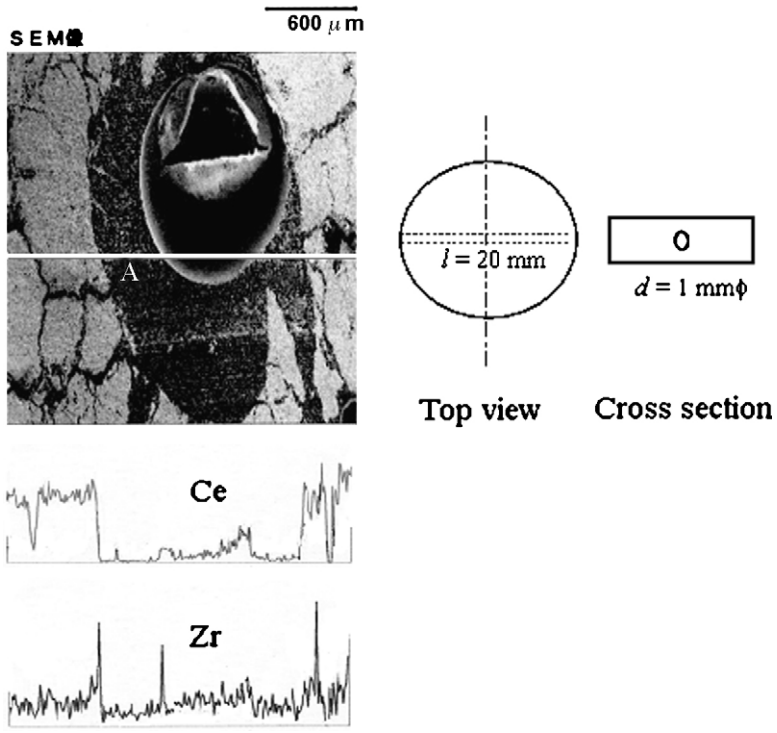

Fig. 1. SEM image and EPMA line analysis of a YSZ film deposited on the wall of a hole through a SDC pellet.

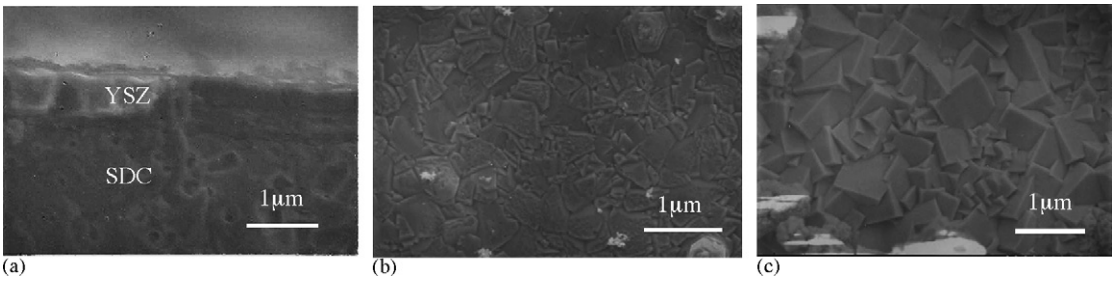

Fig. 2. SEM image of SDC/YSZ composite obtained by the CVI method. (a) The cross-section, (b) the surface of a YSZ film deposited in 20 min and (c) the surface of a YSZ film deposited in 80 min.

allow the Y_2O_3 content of the deposited YSZ film to be controlled with ease. A similar trend was observed in the case of the NiO–ceria pellet reported in our previous paper [17]. The oxygen impurity in argon gas reacts with metal chlorides via:

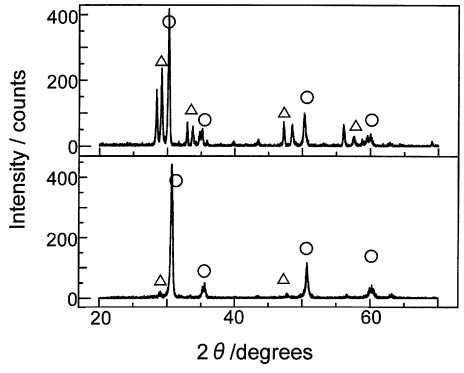

Fig. 3. XRD pattern of YSZ film deposited on SDC pellet: (◯) YSZ, (△) SDC. Carrier gas: Ar (400 ml/min). Deposition time: 20 min (upper), 80 min (lower).

$$ZrCl_4(g) + O_2(g) \rightarrow ZrO_2(s) + 2Cl_2(g) \quad (1)$$

$$2YCl_3(g) + \tfrac{3}{2}O_2(g) \rightarrow Y_2O_3(s) + 3Cl_2(g) \quad (2)$$

The value of free energy at 1273 K for reaction (1) is larger than that for reaction (2) [20]. Thus, the reaction of oxygen with YCl_3 is thought to precede the reaction with $ZrCl_4$ before the metal chlorides reach the substrate giving a low Y_2O_3 content. Since the hydrogen molecules in the carrier gas react with oxygen and suppress reaction (2), controlling the Y_2O_3 content becomes easy.

Table 1
Relationship between Y_2O_3 content and type of carrier gas

Deposition time (min)	Y_2O_3 content (Ar, mol%)	Y_2O_3 content (Ar + 10 ppm H_2, mol%)
20	0.69	5.38
40	0.95	4.12
80	0.77	5.38

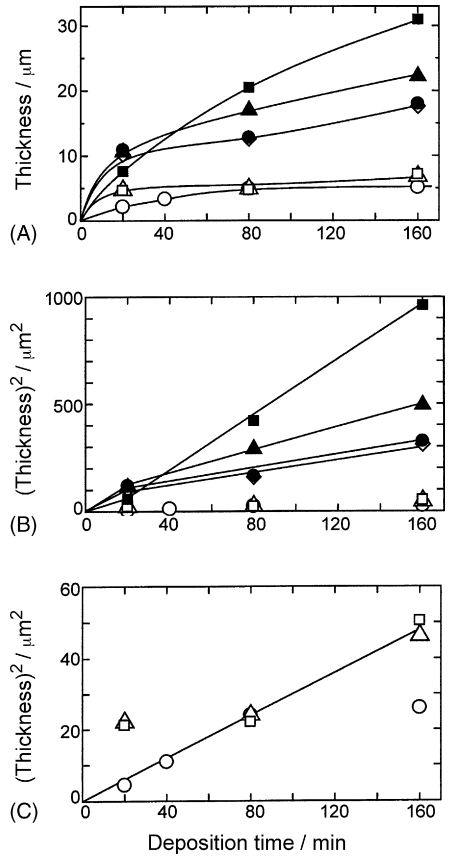

Fig. 4. Effect of NiO content of substrate on the growth rate of YSZ film. Carrier gas: Ar. NiO content (mol%): (◯) 0, (△) 36.5, (□) 60.6, (◇) 69.7, (●) 77.6, (▲) 90.2, (■:) 100. (A) Plots of the thickness of YSZ film vs. the deposition time, (B) plots of the square of the YSZ film thickness vs. the deposition time and (C) plots of the square of the YSZ film thickness vs. the deposition time.

Fig. 4 shows the effect of the NiO content of the substrate on the growth rate of the YSZ film deposited on the SDC substrate. The YSZ film thickness during the first 20 min of deposition was, within experimental error, nearly independent of the NiO content for NiO contents above 69.7 mol%, as shown in Fig. 4A. After this time, the growth rate of the YSZ film decreased, indicating that the growth process changed from CVD to EVD on the NiO pellet, as reported by Inaba et al. [6]. The mechanism of YSZ film growth during the first stage involved reactions between metal chlorides and the NiO–SDC pellet, while during the next stage, reactions occurred between metal chlorides and the oxygen gas derived from the dissociation of the NiO–SDC pellet and the oxygen contained in the carrier argon gas until a gas-impermeable film of YSZ covering the surface of substrate formed, as reported in our previous paper [17]. After the formation of this gas-impermeable YSZ film, the growth mechanism changed from CVD to EVD. The rate-determining step of YSZ growth is well known to be the electrochemical transport of charged species across the YSZ film. Thus, the YSZ growth rate should follow the parabolic law:

$$L^2 = kt, \tag{3}$$

where L denotes the YSZ film thickness, t the deposition time, and k is the parabolic rate constant [21–23]. In the case of the YSZ film, the oxide-ion conductivity is larger than the electronic conductivity (σ_e), and the parabolic rate constant k is derived as:

$$k = \frac{4RTV_M\sigma_e}{2nF^2}[(P^{II}_{O_2})^{-1/4} - (P^{I}_{O_2})^{-1/4}] \tag{4}$$

where V_M is the molar volume, n the number of electrons required for producing one mole of the oxide, F the Faraday constant, R the gas constant, T the deposition temperature, $P^{I}_{O_2}$ the oxygen partial pressure in the NiO–SDC pellet, and $P^{II}_{O_2}$ is the oxygen partial pressure in the reactor. The roughly 0.2 ppm oxygen and 5.3 ppm water in the argon gas reacted with metal chlorides, and was assumed to reach the equilibrium concentration within the operation time of CVI. Thus, the oxygen partial pressure of 1.0×10^{-16} Pa in the CVI apparatus was obtained by calculation [17]. The dissociation pressure of NiO is about 6×10^{-6} Pa at 1273 K [7]. Fig. 4B plots of the square of the YSZ film thickness versus the deposition time. The plots exhibited straight lines at NiO contents above 69.7 mol%, indicating that the growth mechanism of the YSZ film was the EVD process. The slope of the line changed at a deposition time of 20 min, indicating a change in the growth mechanism. The slope increased with increasing NiO content, suggesting that k increased with NiO content. Thus, the value of $P^{I}_{O_2}$ was found to increase with NiO content. The growth rate of the YSZ film did not change appreciably at NiO contents below 60.6 mol%, as shown in Fig. 4A. The plots of the square of the YSZ film thickness versus the deposition time appeared to be linear within a large experimental error, as shown in Fig. 4C. In the first stage of YSZ growth, the CVD process proceeded, and it is thought that the next stage proceeded by the EVD process, but the value of $P^{I}_{O_2}$ seemed to be independent of the NiO content.

The growth rate of the EVD process depends strongly on the oxygen partial pressure in the reactor, $P^{II}_{O_2}$, but changes with the gas-phase reactions (1) and (2). Thus, hydrogen gas was added to the argon in order to decrease $P^{II}_{O_2}$. Fig. 5 shows the effect of the NiO content of the substrate on the growth rate of the YSZ film in the case of the carrier argon gas containing 10 ppm hydrogen gas. $P^{II}_{O_2}$ is obtained by calculation using the assumption that the roughly 0.2 ppm oxygen in the argon gas reacted with the hydrogen gas and metal chlorides, and attained an equilibrium concentration within the operation time of CVI. The value of oxygen partial pressure in the CVI apparatus was 1.0×10^{-24} Pa [17]. The thickness versus time curve was nearly unchanged despite the increase in NiO content from 0 to 60.6 mol%, as shown in Fig. 5A, indicating a single growth mechanism was at play in this region. The plots of the square of the YSZ film thickness versus the deposition time were straight lines, indicating that only the EVD process occurred in this region. Thus, the CVD process using oxygen from the dissociation reactions (reactions (5) and (6)) did not occur:

$$2NiO(s) \leftrightarrows 2Ni(s) + O_2(g) \tag{5}$$

$$4CeO_2(s) \leftrightarrows 2Ce_2O_3(s) + O_2(g) \tag{6}$$

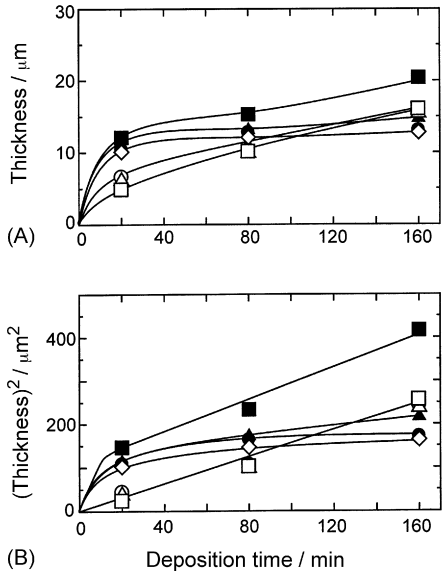

Fig. 5. Effect of NiO content of substrate on the growth rate of YSZ film. Carrier gas: Ar + 10 ppm H_2. NiO content (mol%): (◯) 0, (△) 36.5, (□) 60.6, (◇) 69.7, (●) 77.6, (▲) 90.2, (■:) 100. (A) Plots of the thickness of YSZ film vs. the deposition time and (B) plots of the square of the YSZ film thickness vs. the deposition time.

The EVD process involving the oxygen ion occurred via reactions (7) and (8):

$$O_2 + 4e^- \leftrightarrows 2O^{2-} \quad (7)$$

$$2CeO_2(s) + 2e^- \leftrightarrows Ce_2O_3(s) + O^{2-} \quad (8)$$

These reactions indicate that the oxygen partial pressure of the carrier gas in the reactor is related to the growth mechanism. The growth rate of the YSZ film above 69.7 mol% NiO content was higher than that below 60.6 mol% within during the first 20 min of deposition and decreased suddenly thereafter, as shown in Fig. 5A. The plots did not show straight lines; the slope of the straight lines changed at the deposition time of 20 min, as shown in Fig. 5B. This indicated that the growth process changed at this deposition time. The slope at a deposition time of 80 min increased with increasing NiO content, indicating $P^{I}_{O_2}$ increased with the NiO content in this region. The YSZ film deposited in this region was white, whereas the film deposited below 60.6 mol% NiO content was transparent. This means that the contribution of the CVD process in YSZ film growth increased with the addition of the EVD process at the range above 69.7 mol% NiO content.

Fig. 6 shows the effect of NiO content on the gap between the substrate and YSZ film deposited on the SDC substrate by CVI. We reported that a gap formed between the YSZ film and NiO substrate [7,8] and that the YSZ growth mechanism changed owing to the presence of the gap [17]. The gap decreased from 50 μm to zero as the NiO content dropped from 100 to 60.6 mol%. The substrate shrank with the reduction in the amount of NiO. At 100 mol% NiO, the decrease of volume was estimated to be about 40.7% using the densities of NiO and metal Ni [24]. In the case of 100 mol% CeO_2, a volume increase of about 17.6% was obtained using the densities

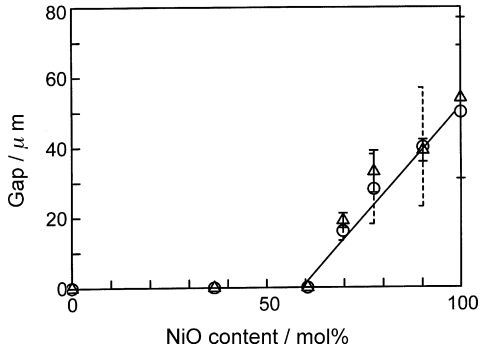

Fig. 6. Gap between substrate and YSZ film deposited on NiO–SDC substrate by the CVI method. Deposition time: 160 min. Carrier gas: (◯) Ar, (△) Ar + 10 ppm H_2.

of CeO_2 and Ce_2O_3 [24]. Thus, the substrate volume gradient changed from negative to positive at a NiO content of about 42.1 mol%, which was estimated through calculations based on the densities. However, the change occurred at about 60 mol% NiO. The observed NiO content at this point was the same as that on the NiO–ceria substrate despite the deviation from the calculated value of 34.6 mol%. The apparent density of the substrate was about 63.3% of the theoretical value and a frame built with SDC at a NiO content below 60 mol% might be kept despite the reduction in NiO content. Thus, the observed value of 60 mol% differed from the calculated value.

Fig. 7 shows the dependence of the YSZ film thickness on the NiO content of the substrate at a deposition time of 160 min during CVI. At NiO contents above 60.6 mol%, the YSZ film thickness obtained in pure argon was larger than that in argon containing 10 ppm hydrogen gas. The CVI method seemed to enhance the CVD process using oxygen in the carrier gas stage, as reported in a previous paper [7,8]. In the case of argon containing 10 ppm hydrogen gas, the YSZ films at NiO contents above 60.6 mol% were thinner than those at NiO contents below 60 mol% since a gap was thought to form that enhanced the dissociation of NiO and the CVD process, while interfering with the EVD process. It is thought that the growth mechanism of YSZ changed at a NiO content of about 60%. Thus, the absence of a gap was thought to suppress the dissociation and to enhance the EVD process. The thickness of the YSZ film at NiO contents below 60.6 mol% obtained in argon gas

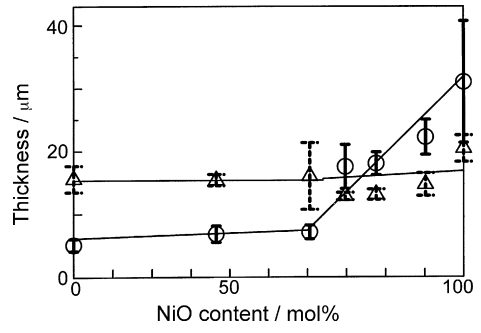

Fig. 7. Dependence of the YSZ film thickness on the content of NiO in the ceria substrate in the CVI method. Deposition time: 160 min. Carrier gas: (◯) Ar, (△) Ar + 10 ppm H_2.

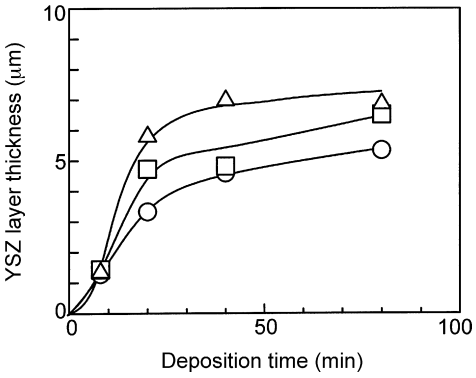

Fig. 8. Dependence of growth rate of YSZ film on SDC thickness. Thickness of SDC substrate (mm); (◯) 1.0, (□) 2.0, (△) 4.0. Carrier gas: Ar + H_2.

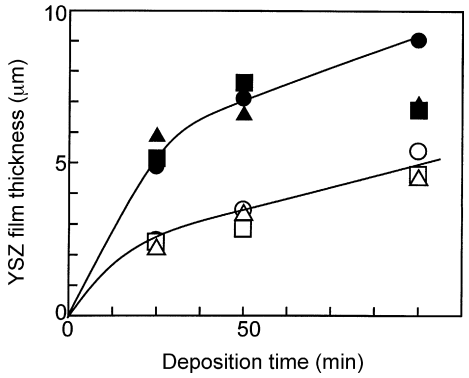

Fig. 9. Effect of flow rate of carrier gas on the growth rate of YSZ films deposited on SDC substrate. Flow rate (ml/min); (◯, ●) 400, (△, ▲) 200, (□, ■:) 100. Open symbols: Ar, solid symbols: Ar + 10 ppm H_2.

decreased slightly with decreasing NiO content since $P^{I}_{O_2}$ was thought to decrease with decreasing NiO content, as reported in our previous paper [17]. The thickness of the YSZ film obtained in argon containing 10 ppm hydrogen gas was larger than that obtained in argon and was almost constant below a NiO content of 60.6 mol%. Below a NiO content of 60.6 mol%, k seemed to be constant since the oxygen partial pressure of the reaction gas was about 10^{-24} Pa and the second term on the right-hand side of Eq. (4) was negligible as compared to first term.

Since $P^{I}_{O_2}$ is determined by reactions (5) and (6), the rate of oxygen supply from the NiO–SDC substrate to the interface of the growing YSZ film affects $P^{I}_{O_2}$. Thus, the effect of the thickness of the SDC substrate on the growth rate of the YSZ film was examined as shown in Fig. 8. The thickness of YSZ films increased with increasing thickness of SDC substrate. In the case of the ceria substrate, the thickness of YSZ film deposited on the ceria substrate was almost unaffected by the change in ceria substrate thickness, as reported in our previous paper [17]. Only the EVD process proceeded during the growth of the YSZ film under these experimental conditions, as discussed in Fig. 5. The thickness of SDC capable of supplying oxygen or oxygen ions to the growing YSZ film was found to be larger than 2.0 mm since the YSZ film thickness increased with increasing SDC substrate thickness. Since $P^{I}_{O_2}$ increased with increasing YSZ film thickness, the diffusion rate of oxygen ions in the SDC substrate was thought to be larger than that in the ceria substrate, as reported by Mineshige et al. [10].

Fig. 9 shows the effects of carrier gas on the growth rate of the YSZ film deposited on SDC substrate. The growth rate of the YSZ film seemed to be almost independent of the flow rate of the carrier gas within experimental error. In the case of the carrier gas of argon containing 10 ppm hydrogen, the oxygen partial pressure in carrier gas was determined by reaction (2) and the following reactions:

$$H_2 + Cl_2 \leftrightarrow 2HCl \quad (9)$$

$$2H_2 + O_2 \leftrightarrow 2H_2O \quad (10)$$

Thus, $P^{II}_{O_2}$ was found to be almost independent of the flow rate of the carrier gas. In the case of pure argon gas, the oxygen partial pressure in the carrier gas increased from 2×10^{-13} to 2×10^{-11} Pa with an increase in the flow rate from 50 to 400 ml min^{-1}, as reported in our previous paper [7]. However, the effect of flow rate on the YSZ film thickness was small, the reason for which remains unclear.

The double layer electrolyte of YSZ/SDC was expected to yield a high SOFC performance. Fig. 10 shows the *V–I* properties for fuel cells using SDC and SDC/YSZ electrolytes. The thickness of the SDC substrate used for YSZ film deposition was 2.0 mm. For a YSZ film thickness of 1.0 μm at 873 K, the *V–I* curve was similar to that of the SDC pellet, as shown in Fig. 10a. The open circuit voltage (OCV) of a 1 μm YSZ film/SDC electrolyte (0.931 V) was larger than that of bare SDC (0.88 V) and less than that of a 4 and 8 μm YSZ/SDC electrolytes. A thin YSZ film coated on the SDC surface prevented the direct contact between SDC and hydrogen gas, suppressing the reduction of SDC. However, the 1 μm-thick YSZ film seemed too thin to suppress the reaction completely. This trend persisted in the tested temperature range from 873 to 1173 K. The slope of the *V–I* curve for a 1 μm YSZ/SDC electrolyte at 973 K was the largest among the tested electrolytes, indicating that it would show the best cell performance (Fig. 10b). The *V–I* curve of 1 μm YSZ/SDC at 1073 K was similar to that of 4 μm YSZ/SDC, but the OCV of the 1 μm YSZ/SDC electrolyte (0.891 V) was lower than that of the 4 μm YSZ/SDC electrolyte (1.027 V) (Fig. 10c). The *V–I* curve of 1 μm YSZ/SDC at 1173 K shifted down because its OCV decreased. The YSZ film of the 1 μm of YSZ/SDC electrolyte was found to behave as a mixed-ion conductor. In the mechanism of YSZ film growth, since metal chloride gases react with the SDC substrate until the formation of a gas-impermeable film during the first stage having a thickness of 1 μm, the YSZ film surface may have cracks. The slope of the *V–I* curves of the 8 μm YSZ/SDC electrolyte was the smallest among the electrolytes tested since the electronic resistance of the YSZ/SDC electrolyte increased with the YSZ film thickness. The 1 μm YSZ/SDC was found to be an effective solid electrolyte in terms of its power generation capacity in the temperature range from 973 to 1073 K. We successfully demonstrated the improvement of cell performance by the fabrication of a YSZ film coated on the surface of SDC by the CVI method.

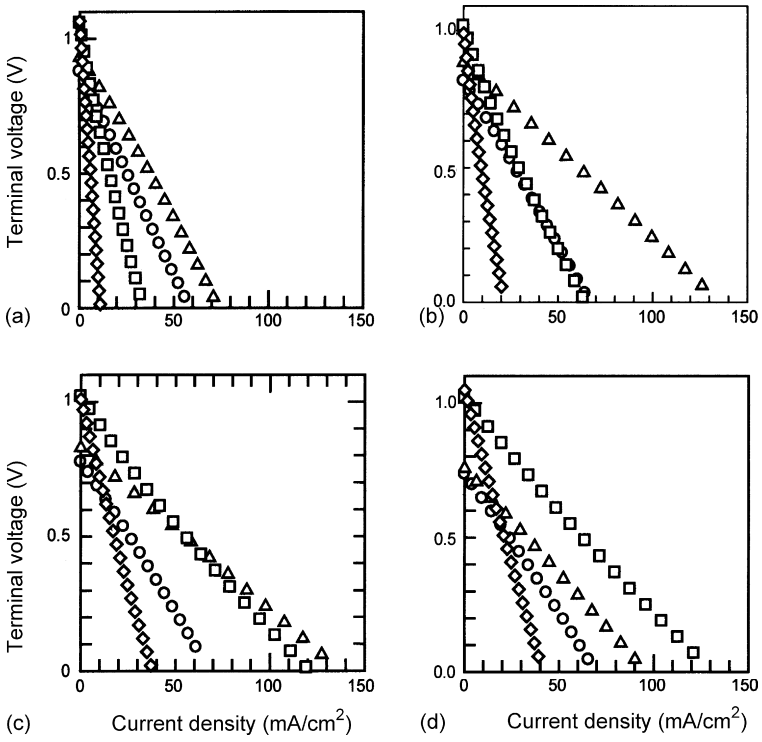

Fig. 10. *I–V* properties of fuel cells using SDC and SDC/YSZ electrolytes. Measurement temperature (K): (a) 873, (b) 973, (c) 1073 and (d) 1173 (◯) the Bare SDC pellet. Thickness of YSZ film (μm): (△)1.0, (□) 4.0, (◇) 8.0. Humidification temperature: 303 K.

4. Conclusion

A dense and strong YSZ film was successfully coated on the NiO–SDC substrate by the CVI method. The main mechanism of YSZ growth was found to be EVD at NiO contents below 60.6 mol%. Our investigation into improving the cell performance through the fabrication of a YSZ/SDC electrolyte by CVI showed that a YSZ film thickness of 1 μm gave the highest cell performance in the temperature range from 973 to 1073 K.

References

[1] Z. Ogumi, T. Ioroi, Y. Uchimoto, Z. Takehara, T. Ogawa, K. Toyama, J. Am. Ceram. Soc. 78 (1995) 593.
[2] M. Inaba, A. Mineshige, S. Nakanishi, N. Nishimura, A. Tasaka, K. Kikuchi, Z. Ogumi, Thin Solid Films 323 (1998) 18.
[3] A. Mineshige, M. Inaba, Z. Ogumi, T. Takahashi, T. Kawagoe, A. Tasaka, K. Kikuchi, J. Am. Ceram. Soc. 78 (1995) 3157.
[4] A. Mineshige, M. Inaba, Z. Ogumi, T. Takahashi, T. Kawagoe, A. Tasaka, K. Kikuchi, Solid State Ionics 86–88 (1996) 251.
[5] M. Inaba, A. Mineshige, T. Maeda, S. Nakanishi, T. Takahashi, A. Tasaka, K. Kikuchi, Z. Ogumi, Solid State Ionics 93 (1997) 187.
[6] M. Inaba, A. Mineshige, T. Maeda, S. Nakanishi, T. Ioroi, T. Takahashi, A. Tasaka, K. Kikuchi, Z. Ogumi, Solid State Ionics 104 (1997) 303.
[7] K. Kikuchi, T. Okaya, W. Hirose, K. Matsuo, A. Mineshige, Z. Ogumi, J. Electrochem. Soc. 150 (2003) C688.
[8] K. Kikuchi, O. Matsuo, A. Mineshige, Z. Ogumi, Solid State Ionics, in press.
[9] T. Inoue, K. Hoashi, K. Eguchi, H. Arai, J. Mater. Sci. 28 (1993) 1532.
[10] A. Mineshige, K. Fukushima, K. Tsukada, M. Kobe, T. Yazawa, K. Kikuchi, M. Inaba, Z. Ogumi, Solid State Ionics 175 (2004) 483.
[11] T. Kudo, H. Obayashi, J. Electochem. Soc. 123 (1976) 415.
[12] K. Eguchi, T. Setoguchi, T. Inoue, H. Arai, Solid State Ionics 52 (1992) 165.
[13] T. Matsui, M. Inaba, A. Mineshige, Z. Ogumi, Solid State Ionics 176 (2005) 647.
[14] Y. Mishima, H. Mitsuyasu, M. Ohtaki, K. Eguchi, J. Electrochem. Soc. 45 (1998) 1004.
[15] T. Tsai, S.A. Barnett, J. Electrochem. Soc. 145 (1988) 1696.
[16] X. Wang, N. Nakagawa, K. Kato, Electrochemistry 70 (2002) 252.
[17] K. Kikuchi, K. Okata, A. Mineshige, J. Power Sources, in press.
[18] L.W. Tai, P.A. Lessing, J. Mater. Res. 7 (1992) 502.
[19] H. Matsumoto, T. Shimura, H. Iwahara, T. Higuchi, K. Yashiro, A. Kaimai, T. Kawada, J. Mizusaki, J. Alloys Compd. 408–412 (2006) 456.
[20] I. Barin, Thermodynamic Data of Pure Substances, VCH, Weinheim, 1993, p. 383, p. 1067.
[21] Y.S. Lin, L.G.J. de Haart, K.J. de Vriers, A.J. Burggraaf, J. Electrochem. Soc. 137 (1991) 3960.
[22] J. Schoonman, J.P. Dekker, J.W. Broerss, Solid State Ionics 46 (1991) 299.
[23] U.B. Pal, S.C. Singhal, J. Electrochem. Soc. 137 (1990) 2937.
[24] David R. Lide (Ed.), CRC Handbook of Chemistry and Physics, 86th ed., CRC Press Taylor & Francis, Boca Raton, 2005, pp. 4–56.